International Journal of
Sustainable Energy Planning and Management

A Non-linear Stochastic Model for an Office Building with Air Infiltration

Anders Thavlov[a] and Henrik Madsen[b]

[a] *Department of Electrical Engineering, Technical University of Denmark, Frederiksborgvej 399, Building 776, 4000 Roskilde, Denmark.*
[b] *Department of Applied Mathematics and Computer Science, Technical University of Denmark, Richard Pedersens Plads, Building 303B, 2800 Kgs. Lyngby, Denmark.*

ABSTRACT

This paper presents a non-linear heat dynamic model for a multi-room office building with air infiltration. Several linear and non-linear models, with and without air infiltration, are investigated and compared. The models are formulated using stochastic differential equations and the model parameters are estimated using a maximum likelihood technique. Based on the maximum likelihood value, the different models are statistically compared to each other using Wilk's likelihood ratio test. The model showing the best performance is finally verified in both the time domain and the frequency domain using the auto-correlation function and cumulated periodogram. The proposed model which includes air-infiltration shows a significant improvement compared to previously proposed linear models. The model has subsequently been used in applications for provision of power system services, e.g. by providing heat load reduction during peak load hours, control of indoor air temperature and for generating forecasts of power consumption from space heating.

Keywords:

Non-linear modelling,
heat dynamic modelling,
stochastic differential equations,
power systems,
air infiltration
URL:
dx.doi.org/10.5278/ijsepm.2015.7.5

1. Introduction

In large-scale power systems with a high penetration of wind power, the intermittent output of the generation side often has a negative impact on the power balance and hence the stability of the power system. Therefore, to counterbalance this intermittency, methods of making the consumption side more flexible are currently being perused. One approach is to use the thermal mass in cold storages to absorb excess power generation from renewable energy sources by temporarily lowering the temperature setpoint. However, the thermal mass of both residential and office buildings can also offer this type of uni-directional energy storage wherever electrical heating is utilised. By allowing the indoor temperature in a typical Danish detached household to vary by one degree around a given reference, a storage capacity of around 10 kWh can be achieved. Such capacity may seem quite modest, but with aggregation of several households a quite large capacity can be utilised. To be able to utilise the potential flexibility from detached buildings, estimates on future power consumption for heating in buildings and future available capacity are required, and hence adequate heat dynamic models of buildings are needed. This paper presents a non-linear model for prediction of the indoor air temperature in an intelligent office building, based on electric heating and weather input.

Adequate models for the heat dynamics of buildings also have applications in other fields. Among these are real-time control of indoor temperature given a varying cost of electricity, e.g. using price signals. Here, heat dynamic models of buildings can be utilised to

*Corresponding author e-mail:

guarantee that the indoor comfort of the residents of the building is not compromised in economic optimisation of electricity consumption. Furthermore, another application is estimation of specific building characteristics like the UA-value of walls and windows and heat capacities. These estimates can be used to form a strategy for how a building can be renovated with respect to energy savings.

The model proposed in this paper is for a specific building called PowerFlexHouse located at the DTU Risø Campus in Denmark. However, the model and estimation technique can be applied to similar types of buildings. So far, the model has been used in several smart grid applications, where flexible demand from PowerFlexHouse is provided within a small power system, see for examples [1] and [2]. Another application of the heat dynamic model is prediction of power consumption from electrical heating, given a weather forecast and an indoor temperature reference.

Following the pioneering work by [3] and [4] on the use of data for modelling the heat dynamics of buildings, several studies have been carried out using linear stochastic differential equations, see for example [5] and [6]. Likewise, several linear models have been proposed for the heat dynamics of PowerFlexHouse, see [7], [8] and [9]. However, none of these studies have included the non-linear effects that the wind has on the convection from the house envelope and on the natural ventilation of the building. Thus, this paper focusses on modelling the heat loss due to natural ventilation as being non-linearly dependent on the wind speed. Likewise, the convection from the house envelope is studied to see if the convection from the surface is non-linear.

To these authors knowledge, no previous work has been carried out in using non-linear stochastic differential equations for modelling the air infiltration in buildings. However, it should be noted that a similar approach has been used to estimate the non-linear heat exchange from photovoltaic modules in [10] and [11].

The outline of this paper is as follows; Section 2 gives an introduction to non-linear stochastic differential equations and parameter estimation. This section also describes PowerFlexHouse, which has formed the basis for data gathering and the building for which the parameter estimation is carried out. Next, a generic model is derived using prior physical knowledge about heat transfer. Section 3 presents the results from the parameter estimation and the model is verified using residual analysis of the model's one step predictions. Finally, in Section 4 the results are discussed together with possible model extensions and applications.

2. Methodology

In this section, an outline is given on how a grey-box approach can be used to formulate a non-linear model for the heat dynamics of an office building. The specific building of interest is an intelligent office building, called PowerFlexHouse, which is located on the DTU Risø campus in Roskilde, Denmark. The method uses non-linear stochastic differential equations to model the dynamics of an observable indoor temperature state variable as well as the non-observable temperature state variables of the electrical space heaters and building envelope. The model is formulated as a lumped model, thus assuming a homogeneously distributed temperature in each of the modelled media. By using a grey-box approach, prior physical knowledge is first used to formulate a set of differential equations. Then statistics on the collected data are used to estimate model parameters, thus combining white-box and black-box modelling. An advantage of this approach is that the physical parameters, i.e. heat capacity and UA-values, are directly given after parameter estimation. This means that the results can be directly compared with results found for similar buildings as well as different types of buildings.

2.1. Model type and parameter estimation

Given a time series of N temperature observations,

$$\mathcal{T}_N = [\boldsymbol{T}_N, \boldsymbol{T}_{N-1}, \boldsymbol{T}_{N-2}, ..., \boldsymbol{T}_0] \tag{1}$$

a mathematical model of the heat dynamics of PowerFlexHouse should be formulated such that the model describes the dynamics as represented by the time series (1). The heat dynamic model will be formulated using non-linear stochastic differential equations. The reason for using stochastic differential equations is to compensate for minor influences not encompassed by the model or unrecognised input, e.g. precipitation or noisy input to the system. Thus, a stochastic process, which accounts for the variations not fully described by a deterministic model, is added to a deterministic model yielding the following set of stochastic differential equations,

$$d\boldsymbol{T}_t = \boldsymbol{f}(\boldsymbol{T}_t, \boldsymbol{u}_t, t, \boldsymbol{\theta}), dt + \boldsymbol{\sigma}(\boldsymbol{u}_t, t, \boldsymbol{\theta}) d\boldsymbol{\omega}_t \tag{2}$$

where $\boldsymbol{f}(\cdot)$ is a non-linear function called the drift term, $\boldsymbol{T}_t$ is a vector containing the modelled temperature states of the building at time t, $\boldsymbol{u}_t$ is a vector containing input to the system and θ is a vector containing the unknown parameters. In the following, the parameters in θ are assumed to be time-invariant and ω_t is assumed to be a standard noise process with independent Gaussian distributed increments, more specifically a Wiener process. $\sigma(\boldsymbol{u}_t, t, \theta)$ is the diffusion term of the process. For an elaborated introduction to stochastic differential equations we refer to [12].

Since only some of the states in (1) are observable, and the sampling is conducted in discrete time, a measurement equation is introduced

$$\boldsymbol{T}_{m,k} = \boldsymbol{h}(\boldsymbol{T}_t, \boldsymbol{u}_t, t, \boldsymbol{\theta}) + \boldsymbol{e}_k \tag{3}$$

where $\boldsymbol{T}_{m,k}$ is the k'th measured output, $\boldsymbol{h}(\cdot)$ is a non-linear function linking the modelled states in (2) with the measured output and $\boldsymbol{e}_k$ is the measurement error. In the following it is assumed that the indoor air temperature state is directly measured, thus $\boldsymbol{h}(\cdot)$ is a linear function picking out the measured temperature states. Hence, (3) simplifies to

$$\boldsymbol{T}_{m,k} = \mathbf{C}\boldsymbol{T}_t + \boldsymbol{e}_k \tag{4}$$

were **C** is a matrix picking out the measured temperature states.

The maximum likelihood estimator has been used as an estimator for θ, which provides the most likely parameter set, $\hat{\theta}$, describing the process observed in $\boldsymbol{T}_{m,k}$ in (3), see [13]. That is, we find parameter estimates such that the likelihood function or the joint probability distribution function is maximised. For a given time series (1) the joint likelihood function is given by

$$\begin{aligned} L(\mathcal{T}_N;\boldsymbol{\theta}) &= p(\mathcal{T}_N \mid \boldsymbol{\theta}) \\ &= p(\boldsymbol{T}_N \mid \mathcal{T}_{N-1}, \boldsymbol{\theta}) p(\mathcal{T}_{N-1} \mid \boldsymbol{\theta}) \\ &= \left(\prod_{k=1}^{N} p(\boldsymbol{T}_k \mid \mathcal{T}_{k-1}, \boldsymbol{\theta}) \right) p(\boldsymbol{T}_0 \mid \boldsymbol{\theta}) \end{aligned} \tag{5}$$

where the rule $P(A \cap B) = P(A|B)\, P(B)$ has been applied N-times to form the joint likelihood function as the product of conditional densities. On the assumption that both ω_t in (2) and $\boldsymbol{e}_k$ in (3) are normally distributed and mutually independent, the conditional density function for a linear model is also normally distributed and thus fully characterised by its mean and variance. In the non-linear case it will be assumed that the conditional densities in (5) are approximately Gaussian and this assumption can be validated. Introducing the innovation or one step prediction error,

$$\boldsymbol{\epsilon}_k = \boldsymbol{T}_k - \hat{\boldsymbol{T}}_{k|k-1} \tag{6}$$

where $\hat{\boldsymbol{T}}_{k|k-1}$ is the estimated mean given by

$$\hat{\boldsymbol{T}}_{k|k-1} = \mathrm{E}\left\{ \boldsymbol{T}_k \mid \mathcal{T}_{k-1}, \boldsymbol{\theta} \right\} \tag{7}$$

and with the covariance

$$\hat{\boldsymbol{R}}_{k|k-1} = \mathrm{V}\left\{ \boldsymbol{T}_k \mid \mathcal{T}_{k-1}, \boldsymbol{\theta} \right\} \tag{8}$$

the likelihood function in (5) can be formulated as

$$L(\mathcal{T}_N;\boldsymbol{\theta}) = \left(\prod_{k=1}^{N} \frac{\exp\left(-\frac{1}{2} \boldsymbol{\epsilon}_k^T \hat{\boldsymbol{R}}_{k|k-1}^{-1} \boldsymbol{\epsilon}_k \right)}{\sqrt{(2\pi)^n \det\left(\hat{\boldsymbol{R}}_{k|k-1} \right)}} \right) p\left(\boldsymbol{T}_0 \mid \boldsymbol{\theta} \right) \tag{9}$$

where $n = \dim(\boldsymbol{T}_m)$. The innovation and covariance in (6) and (8), respectively, can be calculated using an Extended Kalman filter, see e.g. [14] or [15].

2.2. Continuous time stochastic modelling

A procedure for optimisation of (9) with respect to θ has been implemented in the software tool CTSM - *Continuous Time Stochastic Modelling*. CTSM is a computer program for continuous time stochastic modelling, which uses a quasi-Newton method to find the maximum likelihood estimate, $\hat{\theta}$. The software is distributed freely and can be downloaded from the CTSM webpage, [16]. For further information about parameter estimation using CTSM, see [16] and [17].

2.3. Model Validation

It follows from (5) that, for an adequate model, the conditional densities are independent and consequently the one step ahead residuals can be used for model validation. The independence of the residuals can be tested both in the time domain using the auto-correlation function and in the frequency domain using the cumulated periodogram, see [18]. Residual analysis on the proposed models is conducted in Section 3.

2.4. PowerFlexHouse and SYSLAB

PowerFlexHouse is an office building located at the DTU Risø Campus near Roskilde in Denmark. The building has been equipped with various types of sensors and actuators, which allows it to be controlled as a flexible load in the small power system of SYSLAB. SYSLAB is a laboratory and an experimental platform for research in smart-grids and a part of PowerLabDK[1]. Depending on the state of the power system, PowerFlexHouse can postpone or accelerate its energy needs, thus offering power system balance services within SYSLAB.

PowerFlexHouse comprises eight rooms, including a large meeting room in the centre of the building. Each room is individually monitored and controlled and is equipped with a number of different types of sensors and actuators, including

- Temperature sensors
- Motion sensors
- Window- and door sensors
- Actuators for electrical heaters
- Actuators for lighting
- Actuators for opening windows and doors

The sensors and actuators allow the building to be monitored and controlled seamlessly from a house controller. Also, the actuators for the windows, doors and lighting can be used for emulations of residents being present. A picture of PowerFlexHouse and its layout can be seen in Figure 1 (a) and Figure 1 (b), respectively.

In addition to the indoor sensor input, the house controller receives data from a weather mast next to PowerFlexHouse. The weather mast collects data on outdoor temperature, horizontal solar irradiance, as well as wind speed and direction. The collected data is stored in a database together with the indoor sensor states.

A house controller has been developed to handle all communication with sensors and actuators. The controller also implements a high level heat controller for the whole building. Additionally, the house controller is responsible for data acquisition and for storing the house state, i.e. all sensor states, in a database at a sampling rate of 10 seconds. The house controller enables different control strategies to be easily implemented and tested, and currently a number of control strategies have been implemented; from a simple thermostatic controller to a high level model predictive controller that optimises heating over the following 24 hours with respect to a given price signal for the cost of electricity.

The 120 m^2 building is a pavilion-type building, standing freely on concrete slabs, leaving a gap between the ground and the base of the building of approximately 40 cm. The gap has been enclosed with planks. The house is placed such that the south-facing facade, which has a large window area, is turned 17° to the west from direct south. This means that the indoor temperature is highly dependant on the solar irradiance, especially around noon. The width of the outer walls is 170 mm and consists of 100 mm insulation, sandwiched between a plywood facade and interior plasterboards. The inner walls are 70 mm thick and mounted with plasterboards on both sides, sandwiching 50 mm of insulation in-between. The heating for the building comes from ten electrical space heaters, ranging from 750 W to 1,250 W, with a total installed heating power of 9,750 W. For the data generated in this paper, a number of heaters were selected to generate a given total output. The selected heaters were controlled synchronously using a PRBS controller implementing a pre-defined Pseudo-Random Binary Sequence (PRBS). Using PRBS-signals

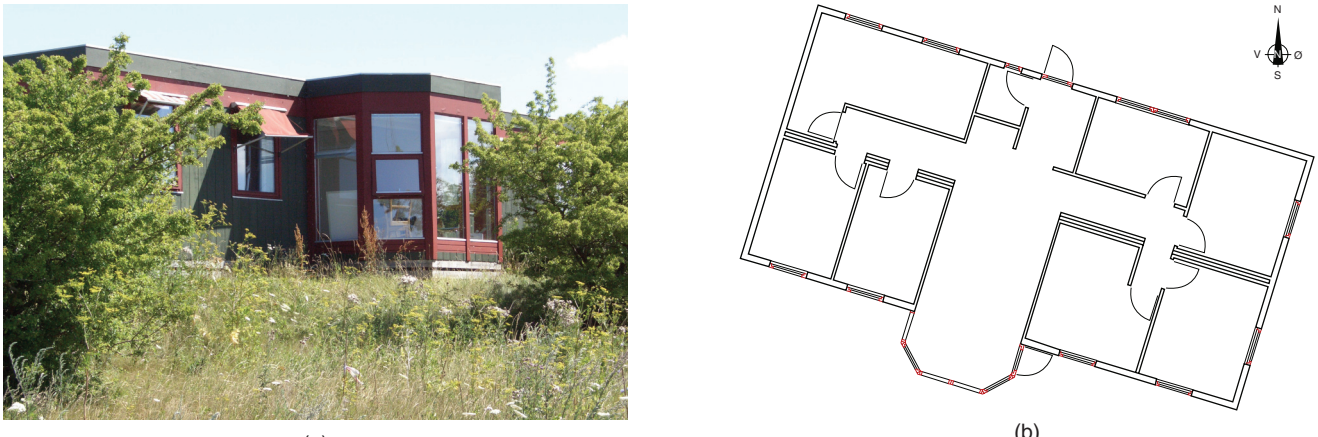

(a) (b)

Figure 1: PowerFlexHouse south facing facade (a) and building layout (b).

[1] http://www.powerlab.dk/

as input to the system ensures optimal conditions for system identification. For a further description about PRBS signals, see [19].

2.5. PowerFlexHouse Model

The heat dynamic model for PowerFlexHouse presented in this paper has three temperature states for the building. These states reflect the temperature of the interior thermal mass, T_i, the average temperature of the ten space heaters, T_h, and the temperature of the building envelope, T_e. Prior physical knowledge is used to formulate a mathematical model of the thermal flow between these three states and the ambient environment. Sub-models for conduction, convection and ventilation are used to compile a total model.

The heaters are hanging freely in the indoor air, thus exchanging heat with the interior media only. The heat transfer is caused by convection from the heater surface. From this the differential equation describing the temperature of the heaters, can be formulated as

$$dT_h = \left(\frac{T_i - T_h}{R_{ih} \cdot C_h} + \frac{\Phi_h}{C_h} \right) dt + \sigma_h \cdot d\omega_1 \tag{10}$$

where C_h is the thermal heat capacity of the heaters, Φ_h is the electrical input and R_{ih} is the convective resistance to transfer heat between the interior thermal mass and the heater.

Likewise, the differential equation describing the temperature of the house envelope is given by,

$$dT_e = \left(\frac{T_a - T_e}{R_{ea} \cdot C_e} + \frac{T_i - T_e}{R_{ie} \cdot C_e} + \frac{A_e \cdot \Phi_s}{C_e} \right) dt + \sigma_e \cdot d\omega_2 \tag{11}$$

where C_e is the thermal heat capacity of the building envelope, R_{ea} and R_{ie} are the thermal resistances related to the combined conductive and convective heat transfer from the envelope to the ambient environment and interior, respectively, T_a is the ambient temperature and A_e is the effective area of the house envelope that is absorbing solar irradiance Φ_s, which is measured on the horizontal plane.

Finally the differential equation for the interior mass is,

$$dT_i = \left(\frac{T_h - T_i}{R_{ih} \cdot C_i} + \frac{T_e - T_i}{R_{ie} \cdot C_i} + \frac{T_a - T_i}{R_{ia} \cdot C_i} + \frac{A_w \cdot \Phi_s}{C_i} \right) dt + \sigma_i \cdot d\omega_3 \tag{12}$$

where C_i is the thermal heat capacity of interior mass, i.e. air, inner walls, furniture, etc. R_{ia} is the resistance to transfer heat directly to the ambient environment, primarily due to natural ventilation of the building, and $A_w \cdot \Phi_s$ is the solar irradiance through the windows, where A_w is the effective size of the windows and Φ_s is the horizontal solar irradiance.

Due to the wind influence on the outside of the building envelope, both the convection from the building envelope and natural ventilation changes from free to forced, hence the resistance to transfer heat can not be assumed to be linear as formulated in (11) and (12), but should instead be a non-linear function of the wind speed. Therefore, in the following the resistances are assumed to take the form,

$$\begin{aligned} R_{ia}\left(W_{spd}\right) &= \frac{1}{k_1 \cdot W_{spd}^{k_2}} \\ R_{ea}\left(W_{spd}\right) &= \frac{1}{k_3 \cdot W_{spd}^{k_4}} \end{aligned} \tag{13}$$

where W_{spd} is the wind speed and $k_x \geq 0$ are unknown parameters to be estimated. For k_2, $k_4 = 0$, we find the linear relation as formulated in (11) and (12). For k_2, $k_4 \neq 0$, both equations in (13) assume the heat transfer to be purely convective and hence conductive heat transfer is neglected. This assumption only holds if the thermal mass of the building envelope is located in the outer surface of the envelope and not inside the walls; however, the approximation is used to investigate whether convective heat transfer is predominant over conduction. Alternatively, a constant term could be added to (13), which would account for the conductive heat transfer.

In Figure 2 the total formulated model, as described by (10) to (12), can be seen as an equivalent RC-network, where electric resistors equal resistance to transfer heat, electric capacitance equals heat capacity, flow of electricity equals flow of heat and voltage differences equal temperature differences. The non-linear resistors have been marked with arrows, indicating varying resistance, i.e. varying with wind speed.

Based on physical knowledge, it can be argued that heat is transferred through the building envelope, but whether the natural ventilation is significant and should be included in the model is a bit more unclear. Therefore different combinations of linear, non-linear and no ventilation, i.e. $R_{ia} = \infty$, have been studied. These results are presented in Section 3.

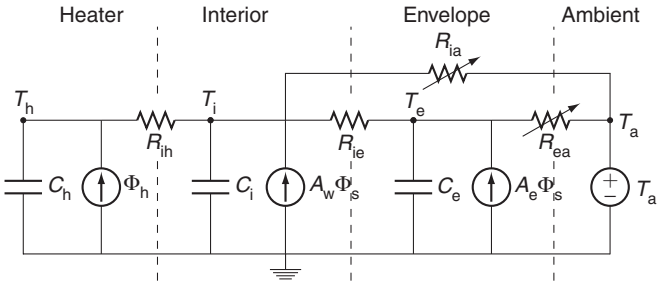

Figure 2: RC-circuit equivalent diagram for the PowerFlexHouse model

Assuming that the indoor measured temperature is a direct representative for the interior state temperature, the model takes the form,

$$
\begin{aligned}
dT_i &= \left(\frac{T_h - T_i}{R_{ih} \cdot C_i} + \frac{T_e - T_i}{R_{ie} \cdot C_i} + \frac{T_a - T_i}{R_{ia}(W_{spd}) \cdot C_i} + \frac{A_w \cdot \Phi_s}{C_i} \right) \\
&\quad dt + \sigma_1 \cdot d\omega_1 \\
dT_h &= \left(\frac{T_i - T_h}{R_{ih} \cdot C_h} + \frac{\Phi_h}{C_h} \right) dt + \sigma_2 \cdot d\omega_2 \\
dT_e &= \left(\frac{T_a - T_e}{R_{ea}(W_{spd}) \cdot C_e} + \frac{T_i - T_e}{R_{ie} \cdot C_e} + \frac{A_e \cdot \Phi_s}{C_e} \right) \\
&\quad dt + \sigma_3 \cdot d\omega_3 \\
T_{m,k} &= T_i(k) + e_k
\end{aligned}
\tag{14}
$$

where $R_{ia}(W_{spd})$ and $R_{ea}(W_{spd})$ can take the form as either linear or non-linear as defined in (13). Also, $R_{ia}(W_{spd}) \to \infty$ for $W_{spd} \to 0$, implying no heat transfer due to natural ventilation.

2.6. Data

Four experiments were conducted in PowerFlexHouse in the period from February to March 2008. The purpose of the experiments was to collect data for model parameter estimations. The only input to the system in (14) that can be directly manipulated is the heat input from the electrical space heaters. The heaters were controlled synchronously, i.e. all heaters were on or off in the same time instance, using a binary signal generated as a Pseudo Random Binary Sequence. A different PRBS signal was generated for each experiment and each signal was designed such that the heat input from the electrical space heaters would excite the temperature states in the time domain around where time constants were expected to be found. The number of heaters being controlled was chosen such that the temperature in any room would not exceed 30 ^{0}C at any time during the experiment. This was done to prevent the house controller from being overridden by the internal space heater thermostat which only allows room temperatures up to 30 ^{0}C, after which the heater switches off. The time series of the observed interior temperature $T_{m,k}$, ambient temperature T_a, heat input Φ_h and solar irradiance Φ_s are plotted in Figure 3.

The dynamics of the interior temperature state can be seen to vary with the external input. Especially the PRBS-controlled heat input can be seen in the variation of the interior temperature. Also, the effects from the daily variation in ambient temperature and solar irradiance can be clearly seen in the figures.

Wind data was also collected during the four experiments. The wind speed and direction are depicted in Figure 4, where the wind measurements are plotted.

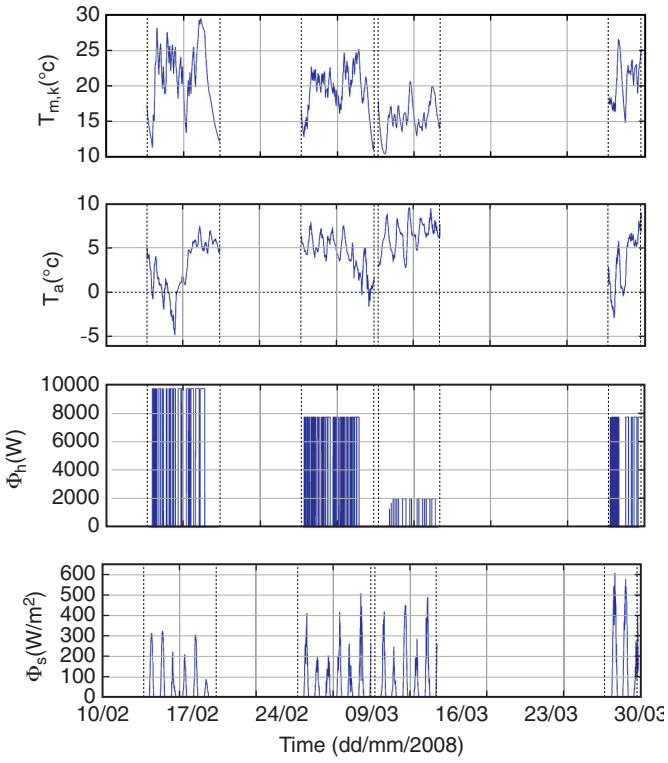

Figure 3: Input to the dynamic system formulated in (2) for parameter estimation.

Each dot in the figure represents the direction from which the wind is blowing. The plot shows that the wind in the period of the experiments came mainly from the west, with measured wind speeds of up to 25 m/s. To remove high order frequency variations, the wind speed and direction have been filtered with a low-pass filter.

The model of the interior temperature, i.e. (12), only takes one indoor temperature, i.e. T_i. As a representative temperature, the average indoor air temperature of the eight rooms has been used. Instead of weighing the temperatures equally, other weights could have been applied to weight larger rooms higher. For example, this could have been done using principal component analysis; however, no significant improvement in log-likelihood has been observed using different weights.

3. Results

This section presents the model parameter estimates for four different non-linear models and compares the results with previously proposed linear models from [8] and [7]. The maximum of the log-likelihood for the non-linear models is compared to the log-likelihood found for similar linear models Also, the best performing model is verified in both the time domain and frequency domain.

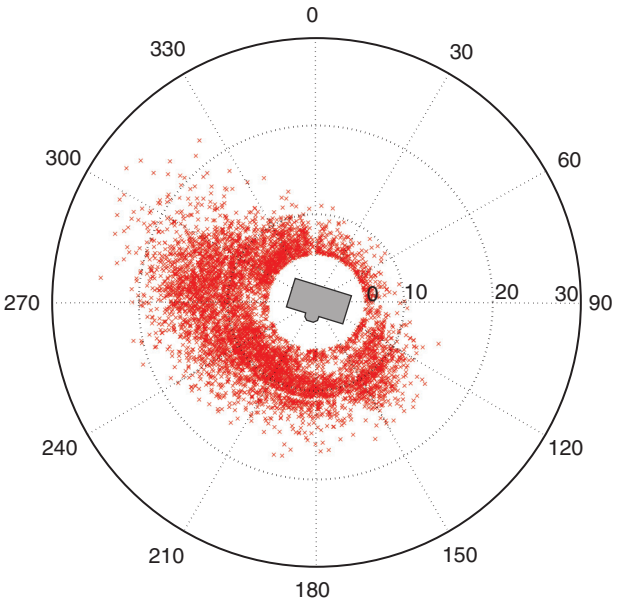

Figure 4: Wind rose data collected during the experiments sampled at intervals of 5 minutes. The wind direction relative to the house can be deducted from the outline of PowerFlexHouse in the middle of the plot.

3.1. Parameter Estimates

Six different combinations of non-linear and linear heat transfer, with and without air infiltration, were examined and model parameters estimated for each model. The parameter estimates, together with their respective standard deviations, are presented in Table 1. In the table, the models have been named Model A to F, where Model A is the linear reference model as presented in [7], Model B is a linear reference model with natural ventilation presented in [8] and Model C to F are non-linear variations of Model A and B.

The table shows that the parameter estimates are much alike for the six models, except R_{ia} for Model B and E. As seen from the table, the two estimates are both associated with a relative high standard deviation, signifying that they could potentially be the same. Likewise, the relative standard deviations on R_{ih} and C_h are quite high, thus implying that the modelling uncertainty on T_h is high and that the model therefore can not be used to estimate the temperature of the space heaters. However, together these two estimates simply imply a fast transfer of heat from the heater to the indoor air, i.e. a fast discharge of the capacitor.

The highest log-likelihood is achieved by Model C and F, were the natural ventilation is non-linear and the convection from the envelope is modelled as linear and non-linear, respectively.

Since the linear models are sub-models of the non-linear models, a statistical test can be used to verify whether the increase in log-likelihood is significant or not. For this, Wilk's likelihood ratio test can be used, see [20]. The test is given by,

$$\lambda = -2(\mathrm{LL}_0 - \mathrm{LL}_1) \tag{15}$$

where LL_0 and LL_1 is the log-likelihood for the sub-model and sufficient model, respectively. As the number of observations increases, λ converges to a χ^2-distribution with k-degrees of freedom, where k is the difference in number of model parameters for the two models. From this, the p-values in Table 1 have been found. The log-likelihood values show that all the non-linear models are significantly better than the linear models, and that Model C and F have the lowest p-values, when compared to Model A.

For Model C and F, the model estimates for k_1 and k_2 are almost the same. Plotting the resistance to natural ventilation R_{ia} using (13) reveals that the resistance is

Table 1: Model parameter estimates and their respective standard deviation noted in brackets.

Name	Model A	Model B	Model C	Model D	Model E	Model F
R_{ia}	∞	Linear	Non-linear	∞	Linear	Non-linear
R_{ea}	Linear	Linear	Linear	Non-linear	Non-linear	Non-linear
Coefficient			**Estimates**			
A_e, [m^2]	23.15	22.64	20.93	21.37	21.02	21.09
	(3.91)	(3.60)	(3.00)	(2.86)	(2.90)	(3.01)
A_w, [m^2]	9.66	9.55	9.52	9.23	9.15	9.48
	(0.70)	(0.80)	(0.67)	(0.61)	(0.68)	(0.70)
C_e, [kWh/°C]	8.12	7.81	6.64	7.14	6.93	6.69
	(1.03)	(1.18)	(0.79)	(0.74)	(0.81)	(0.79)
C_h, [kWh/°C]	0.000367	0.000367	0.000370	0.000372	0.000372	0.000371
	(0.000526)	(0.000569)	(0.000359)	(0.000534)	(0.001780)	(0.000574)
C_i, [kWh/°C]	2.48	2.48	2.46	2.45	2.45	2.46
	(0.06)	(0.06)	(0.06)	(0.06)	(0.06)	(0.06)
R_{ea}, [°C/kW]	2.24	2.48	2.91	–	–	–
	(0.16)	(0.67)	(0.33)	(–)	(–)	(–)
R_{ie}, [°C/kW]	0.83	0.85	0.87	0.81	0.82	0.87
	(0.04)	(0.06)	(0.05)	(0.04)	(0.05)	(0.05)
R_{ia}, [°C/kW]	–	40.33	–	–	51.35	–
	(–)	(100.99)	(–)	(–)	(63.03)	(–)
R_{ih}, [°C/kW]	898.27	898.35	898.42	898.15	898.37	897.45
	(1287.80)	(1389.20)	(875.97)	(1287.90)	(4289.10)	(1384.20)
$k_1(R_{ia})$	–	–	0.0141	–	–	0.0152
	(–)	(–)	(0.0113)	(–)	(–)	(0.0110)
$k_2(R_{ia})$	–	–	0.9032	–	–	0.9366
	(–)	(–)	(0.2880)	(–)	(–)	(0.3168)
$k_3(R_{ea})$	–	–	–	0.3353	0.3053	0.3343
	(–)	(–)	(–)	(0.0314)	(0.0488)	(0.0385)
$k_4(R_{ea})$	–	–	–	0.1857	0.1954	0.0391
	(–)	(–)	(–)	(0.0486)	(0.0575)	(0.0632)
Log-likelihood	9242.27	9242.32	9256.94	9247.23	9247.23	9257.09
Parameters	15	16	17	16	17	18

p-value	Model A	Model B	Model C	Model D	Model E	Model F
Model A	–	0.751	4.25×10^{-7}	1.68×10^{-3}	6.96×10^{-3}	1.64×10^{-6}
Model B	–	–	6.39×10^{-8}	–	1.71×10^{-3}	3.85×10^{-7}
Model C	–	–	–	–	–	0.585

very dependent on the wind speed as seen in Figure 5, where also the obtained constant estimate from Model B is plotted. Likewise, a plot of the non-linear R_{ea} from Model F, together with the constant estimate from Model B are presented.

The plot shows that R_{ia} is much more dependent on the wind speed than R_{ea}, and that the non-linear estimates are close to their respectively constant estimates, as obtained in Model B, for wind speeds around 2–3 m/s, which is quite close to the average measured wind speed. Furthermore, R_{ia} increases rapidly when the wind speed goes towards zero. Hence, it can be concluded that for wind speeds below 5 m/s, the heat loss due to ventilation is quite small compared to conduction through the envelope. For wind speeds around 20 m/s, the resistance is approximately of the same size as the heat loss through the envelope, and as the wind speed increases the resistance drops and the air infiltration becomes the dominant factor in the heat loss of the building. This is consistent with the theory for natural ventilation. Furthermore, from the plot is seen that R_{ea} is nearly constant relative to R_{ia} which implies that the heat transfer through the envelope is approximately linear and hence behaves like conductive heat transfer. This further strengthens the argument for Model C being the most adequate model.

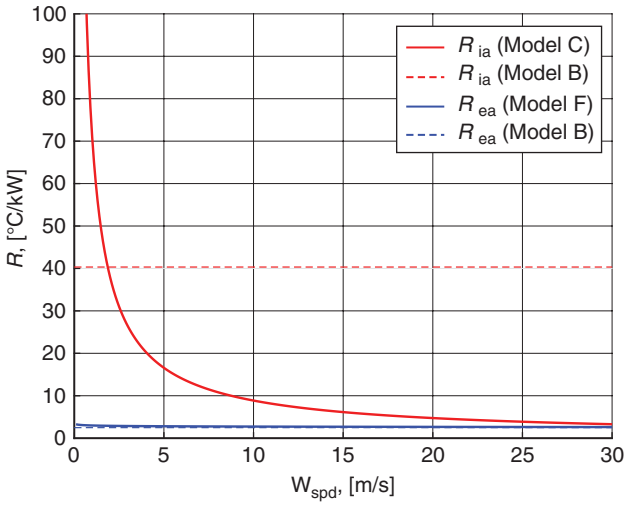

Figure 5: Comparison between the convective resistance through the building envelope, R_{ia}, and from the outside surface, R_{ea}, versus wind speed, W_{spd}.

3.2. Model Validation

The formulation of the model in Section 2 assumed that ω_t is independent for non-overlapping time intervals and that $\boldsymbol{e}_k$ is white noise. Hence, the residuals for the one step prediction in (6) should resemble white noise. Using tests in both the time domain and frequency domain, all the non-linear models have been validated. In Figure 6, the auto-correlation function is plotted for the one step predictions for Model C. The auto-correlation function shows some correlation at lags 1 and 4, which fall outside the 95% confidence interval; however, they are still quite small, hence indicating that the residuals do resemble a white noise process.

Also the spectrum for Model C is seen to be approximately equally distributed over all frequencies, which is also apparent from the cumulated periodogram, where the cumulated periodogram is seen to fall within the 95% confidence interval, except around 0.4, where the confidence interval is broken. The exact cause of this has not been identified, but could be caused by the time delay from the propagation of heat in the temperature sensor; hence, the temperature sensor should be modelled separately using an additional temperature state. The three plots in Figure 6 imply that the model can certainly be improved, but also that the residuals to a large extent do resemble a white noise process and that Model C thus gives an adequate description of the heat dynamics of PowerFlexHouse.

4. Discussion

The study presented in this paper has shown that non-linear stochastic differential equations can be used to describe the non-linear effects caused by forced ventilation or infiltration in a thermally light building. A parameter estimation technique for a non-linear state space model has been demonstrated for a specific building, based on data collected in the office building and from a weather mast on-site.

From the p-values in Table 1, it can be seen that the non-linear models are significantly better than any previous linear models of the heat dynamics of PowerFlexHouse as suggested in [7] and [8]. Also from the log-likelihood estimates it can be seen that Model C and F achieve the highest log-likelihood. However, with an equally high log-likelihood and with one additional parameter in Model F, it can be concluded that Model C, with 16 parameters, is sufficient to describe the heat dynamics of PowerFlexHouse. Also, the correlation matrix of the estimates for Model F has off-diagonal values close to one, which implies that the model is over-parameterized. This further supports that Model C is the best performing model. Additionally it is seen that with an increasing number of parameters in the model, the log-likelihood is seen to stagnate, which further confirms that the model becomes over-parameterized and that 16 parameters are sufficient to describe the heat dynamics.

Unfortunately, no building data is available for PowerFlex-House that could confirm whether the parameter estimates are correct. However, the estimates can be compared to expected building data given by building regulations from the time of construction, to see whether they comply with the requirements. For example, the required u-values at time of construction were $u_{window} = 2.90$ W/(°Cm^2) and $u_{wall} = 0.40$ W/(°Cm^2) for windows and walls respectively. By approximating the surface of PowerFlexHouse with a rectangular box with dimension 15 m × 8 m × 3 m, the total surface of the building is A = 378 m^2 of which approximately 27 m^2 are windows. From this, the weighted u-value of the whole building can be calculated as:

$$u = \frac{(378-27)\mathrm{m}^2 \cdot 0.40\mathrm{W}/\left(^\circ\mathrm{C\,m}^2\right) + 27\mathrm{m}^2 \cdot 2.90\mathrm{W}/\left(^\circ\mathrm{C\,m}^2\right)}{378\mathrm{m}^2}$$
$$= 0.58\mathrm{W}/\left(^\circ\mathrm{C\,m}^2\right)$$

Furthermore, by assuming a wind speed of 3 m/s giving R_{ia} = 23.6°C/kW and a steady state in the heat

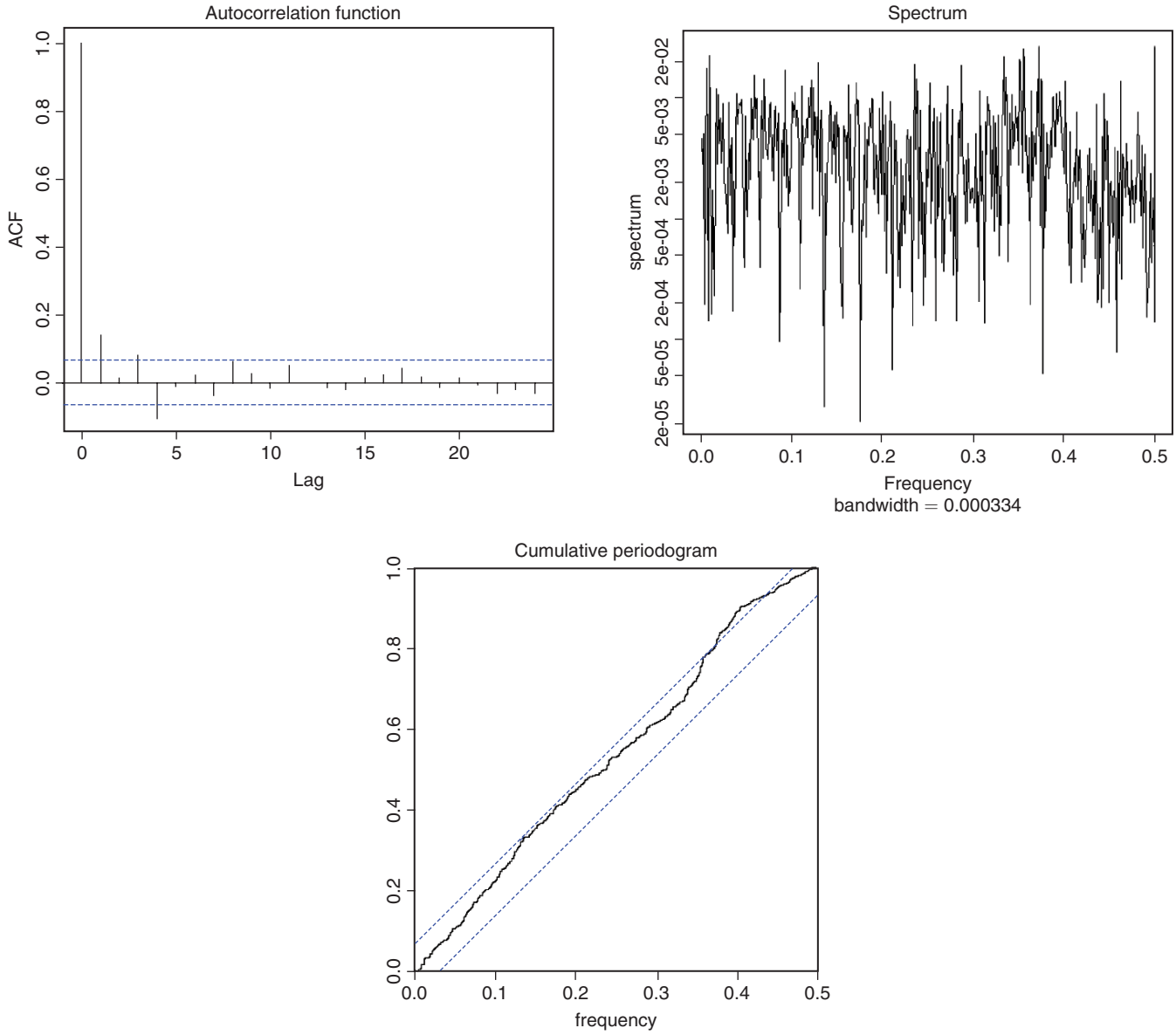

Figure 6: Auto-correlation, spectrum and cumulated periodogram for the one step prediction for Model C.

transfer from the building, the total thermal resistance from the building can be calculated as,

$$R = \frac{1}{1/R_{ia} + 1/(R_{ie} + R_{ea})} = \frac{1}{1/23.6 + 1/(2.91 + 0.87)} = 3.26\,°\text{C}/\text{kW}$$

which is equivalent to a u-value around 0.8W/(°Cm^2) $\left(u = \frac{1}{R \cdot A}\right)$. Considering the wear of the building envelope, including draughty air registers, the estimated value is not far from what was required by the building regulations at the time of construction. Moreover, the total heat capacity of the building is estimated to around 9 kWh/°C, which is equivalent to 75 Wh/(°C m$^{2)}$. This value falls in the range of what is characterised as thermally light buildings, which is expected considering the light construction materials that the building is composed of. Finally, the window area of PowerFlexHouse is approximately 27 m^2. Assuming that the effective window area is approximately 60% of the real window area, as were used in [5], the estimates of A_w are also close to what would be expected.

4.1. Model Extensions

During this study it was also investigated whether the model could be improved by projecting the wind vector onto the orthogonal of each surface of the building. This, however, would require an additional six parameters in the model, which makes the model highly over-parameterized and reasonable parameter estimation impossible. As an alternative approach the model parameters were estimated four times using the projected wind speed as the basis for parameter estimation, instead of the general wind speed. This revealed that a slightly higher log-likelihood could be achieved when using the wind speed projected on the south-ward direction, indicating a higher sensitivity to south-ward wind compared to the other directions. It can be argued that the result is reasonable, since PowerFlexHouse is sheltered from the north and east by other buildings and to the west by trees and bushes. However, another argument against the model extension could be that the model estimates come from a data-set where the wind has mainly been blowing from the west. The decision whether the first or second argument holds is left for another study.

4.2. Applications

As stated in Section 1, the model is used in a heat controller to ensure indoor comfort and to predict power consumption. However, the model technique presented in this paper can be applied in many other areas; for example for estimating specific building parameters which are directly given by the estimation technique, or for estimation of a given building's annual energy need for heating. Furthermore, the model can also be used to estimate heat loss due to air infiltration though the envelope. Assuming steady state in the envelope, i.e. no net flow into the envelope, and a temperature difference at 10°C over the envelope, the heat loss distribution between the infiltration loss and loss through the envelope can be calculated. This is presented in Table 2, where the heat loss due to natural ventilation increases rapidly for wind speeds over 10 m/s and for a wind speed above 25 m/s, 50% of the total heat loss is due to ventilation.

The results presented in Table 2 show that natural ventilation should be minimised, e.g. by closing air vents or registers when the wind speed increases above 10–15 m/s. At present, the air registers in PowerFlexHouse are manually controlled, but installing actuators to close the registers when the wind speed reaches a given threshold would greatly reduce heat loss due to air infiltration. However, this type of control would change the dynamics of the heat transfer through the house envelope and another functional description of R_{ia} should most likely be used. An investigation of the heat transfer as a function of the state of the air registers is left as a subsequent study.

Table 2: Percent-wise heat loss due to natural ventilation and through building envelope.

Wind speed, [m/s]	10	20	30
R_{ia}, [°C/kW]	8.86	4.74	3.29
$R_{envelope}$, [°C/kW]	3.78	3.78	3.78
Ventilation heat loss, [%]	29.90	44.37	53.50
Envelope heat loss, [%]	70.10	55.63	46.50

Acknowledgement

The work was partly funded by DSF (Det Strategiske Forskn-ingsråd) through the ENSYMORA (DSF No. 10-093904) project, which is hereby acknowledged.

References

[1] Y. Zong, D. Kullmann, A. Thavlov, O. Gehrke, H. W. Bindner, Application of model predictive control for active load management in a distributed power system with high wind penetration, Transactions on Smart Grid, IEEE 3 (2012) 1055–1062.

[2] A. Thavlov, H. Bindner, Utilization of flexible demand in a virtual power plant set-up, IEEE Transactions on Smart Grid 6 (2) (2015) 640–647. doi:10.1109/TSG.2014.2363498.

[3] R. Sonderegger, Diagnostic tests to determine the thermal response of a house, ASHRAE Transactions 91.

[4] A. Rabl, Parameter estimation in buildings; methods for dynamic analysis of measured energy use, Journal of Solar Energy Engineering 110 (1988) 52–66.

[5] H. Madsen, J. Holst, Estimation of continuous-time models for the heat dynamics of a building, Energy and Buildings 22 (1995) 67–79.

[6] K. K. Andersen, H. Madsen, L. H. Hansen, Modelling the heat dynamics of a building using stochastic differential equations, Energy and Buildings 31 (2000) 13-24.

[7] P. Bacher, H. Madsen, Identifying suitable models for the heat dynamics of buildings, Energy and Buildings 43 (2011) 1511–1522.

[8] A. Thavlov, Dynamic optimization of power consumption, Master's thesis, DTU IMM, Technical University of Denmark (2008).

[9] A. Thavlov, H. W. Bindner, A heat dynamic model for intelligent heating of buildings, International Journal of Green Energy 12 (3) (2015) 240–247. doi:10.1080/15435075.2014.891516.

[10] M. Jiménez, H. Madsen, J. Bloem, B. Dammann, Estimation of non-linear continuous time models for the heat exchange dynamics of building integrated photovoltaic modules, Energy and Buildings 40 (2008) 157–167.

[11] N. Friling, Stochastic modelling of building integrated photovoltaic modules, Master's thesis, Informatics and Mathematical Modelling, Technical University of Denmark, DTU, Richard Petersens Plads, Building 321, DK-2800 Kgs. Lyngby (2006).

[12] B. Øksendal, Stochastic Differential Equations, 4th Edition, Springer, Berlin, 1995.

[13] N. R. Kristensen, H. Madsen, S. B. Jørgensen, Parameter estimation in stochastic grey-box models, Automatica 40 (2) (2004) 225–237. doi:10.1016/j.automatica.2003.10.001.

[14] A. H. Jazwinski, Stochastic Processes and Filtering Theory, Academic Press, New York, 1970.

[15] P. S. Maybeck, Stochastic Models, Estimation and Control; Vol 1,2,3, Academic Press, New York, 1982.

[16] Continuous Time Stochastic Modelling webpage, *http://www.ctsm.info.*

[17] N. R. Kristensen, H. Madsen, CTSM 2.3 - Mathematics Guide. URL *http://www2.imm.dtu.dk/ctsm/MathGuide.pdf*

[18] H. Madsen, Time Series Analysis, Chapman & Hall, 2008.

[19] K. R. Godfrey, Correlation methods, Automatica 16 (1980) 527-534.

[20] H. Madsen, P. Thyregod, An Introduction to General and Generalized Linear Models, Chapman & Hall, 2011.